ACS APPLIED MATERIALS & INTERFACES

Research Article

www.acsami.org

Facile Fabrication and Magnetic Properties of a One-Dimensional Magnetite Peapod in a Lipid Nanotube

Youn-Gyu Han,* Masaru Aoyagi,* Masumi Asakawa, and Toshimi Shimizu

Nanotube Research Center (NTRC), National Institute of Advanced Industrial Science and Technology (AIST), Tsukuba Central 5, 1-1-1 Higashi, Tsukuba, Ibaraki 305-8565, Japan

Supporting Information

ABSTRACT: Magnetite nanoclusters (MNCs) were aligned one-dimensionally in the hollow cavity of a lipid nanotube (LNT) as a peapod using a simple mixing method in an aqueous solution. The electrostatic interaction of the two materials was considerable enough to allow the preparation of a densely packed MNC-LNT peapod composite. The composite was formed at a pH 5.4–6.8, i.e., near the isoelectric point of the MNCs. At a pH 5.4–6.8, there was neither a strong attractive nor repulsive electrostatic interaction between the surface of the MNC and the LNT. The MNCs-capped LNT composites were formed at basic conditions (above a pH 7.8) in which the MNCs and the LNT pushed each other because of their opposite surface charges. The magnetic property measurement revealed that the 1D aligned MNCs in the peapod structure had a much higher coercivity (10.6 Oe) than the bulk randomized MNCs (5.8 Oe).

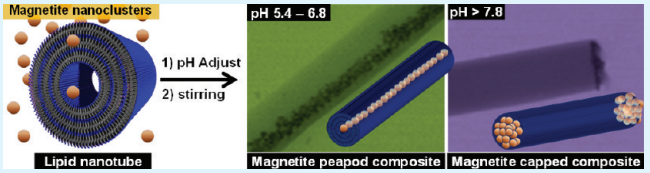

KEYWORDS: *1D nanostructure, magnetic nanotube, lipid nanotube, magnetite, peapod, nanowire*

INTRODUCTION

Some amphiphile lipid molecules such as glycolipids, phospholipids, and peptide lipids self-assemble into open-ended, hollow cylindrical structures in dispersed media.[1−4] Lipid nanotubes (LNTs) have a few advantages such as a controllable diameter and length, a tunable surface property, and a flexibility that is unlike that of a carbon nanotube and an inorganic nanotube. The hollow cylinder space of the LNT has drawn much attention due to its potential application as a capsule or a one-dimensional (1D) template.

The encapsulation ability of LNT has been examined by filling the hollow space with aqueous dispersions of guest materials such as liposome, DNA, protein, ferritin, gold, or silver nanoclusters.[5−12] It was reported that the capillary force played a key role in the introduction of the guest materials into the LNT. Also, a research showed that negatively charged latex beads were encapsulated in the positively charged inner surface by electrical attraction without a capillary diffusion force. Not much attention has been given to the surface electrostatic interactions between metal nanoclusters and the LNT, though. Also, in most cases, the nanoclusters filled only a short length (<1 μm) in the cavity of the LNT.[9−11]

The guest particles form 1D aligned assemblies in the LNT that make the LNT look like a peapod. The composites are assumed to show properties of 1D materials such as nanowires. Theoretically, closely packed conducting clusters will show electrical properties that are similar to those of conducting nanowires.[13] 1D aligned magnetic clusters are similar to magnetic nanowires. They or their hybrid composites with other functional materials will be the building blocks of future nanodevices such as semiconductors, magnetic and photonic nanodevices, and molecular nanodevices in functional circuits and chips.[14−16] These devices will require facile techniques for establishing electrical contact between the nanoentities and their supporting substrates for applications in electronics, optoelectronics, sensors, spintronics, and thermoelectric devices. Conventional methods of preparing 1D materials are electro-deposition or synthesis of nanoclusters on linear templates, electrospinning, etc.[18,19] Compared to the 1D aligned nanoclusters, these materials may require sophisticated equipment and processes and expensive precursor materials. Thus, to reduce the energy requirement for materials production, a simple and low-energy process of preparing 1D aligned nanomaterials must be developed.

LNT composites and inorganic 1D materials significantly differ in their flexibility. The 1D morphology of the composites could be transformed by external forces such as applied force, magnetic force, and electrical force. Thus, the 1D composites with aligned nanoclusters have been expected to be applicable to flexible elements for electronic, photonic, and magnetic devices.[20−22] A report evaluated the flexibility of a lipid microtube (with a large hollow space) that contained Fe_2O_3 magnetic nanoparticles.[23] They did not examine the change in the magnetic property after the encapsulation of the particles, though.

In this study, a simple and high-yield method of preparing magnetite peapod composites as 1D magnetic nanomaterials was demonstrated. The electrostatic surface interactions

Received: January 21, 2012
Accepted: April 10, 2012
Published: April 10, 2012

   dx.doi.org/10.1021/am300122f | ACS Appl. Mater. Interfaces 2012, 4, 2439–2444

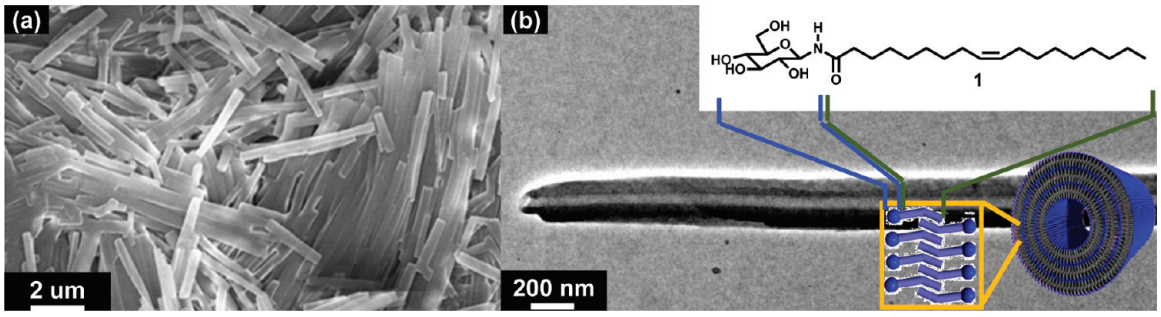

Figure 1. (a) SEM and (b) TEM images of the LNT, and schematic of the LNT and molecular structure of the glycolipid (**1**).

between the guests (the magnetite nanoclusters or MNCs) and the host (LNT) were considered for the preparation of the peapod composite, contrary to previous studies.[9−11] The MNCs filled the majority of the cylindrical space of the LNT. The magnetic property of the 1D aligned MNCs was also compared with that of the randomized bulk MNCs.

EXPERIMENTAL DETAILS

Materials. $FeCl_2{\cdot}4H_2O$, $FeCl_3{\cdot}6H_2O$, HCl (36% w/w aq. soln.) and ammonia (28% w/w aq. soln.) were purchased from Wako Chemical. All the purchased chemicals were reagent-grade and were used without further purification. Ultrapure water was used for all the experiments. Glycolipid (1), N-(9-cis-Octadecenoyl)-β-D-glucopyranosyl-amine was synthesized and self-assembled into LNT according to the aforementioned methods.[1,24] The prepared glycolipid was pale-yellow, however, and its aqueous solution was acidic. This was caused by some impurities due to the incomplete purification. Therefore, further purification was needed. The purification method was as follows: 20 g of the synthesized material was dissolved in 200 mL of methanol with 4 g of silica gel and 1 g of activated charcoal at 60 °C. After the silica and the charcoal were removed via filtration, the clear filtrate was cooled to room temperature. The precipitated LNTs were filtered and washed with ultrapure water (50 mL for 3 times) until the aqueous dispersion of the LNTs had a neutral pH and their conductivity dropped to less than 10 μS/cm.

Preparation of the Raw MNC and the MNC-LNT Peapod Composites. An aqueous suspension of the raw MNCs was prepared using the typical method.[25,26] Briefly, an aqueous solution of 0.099 g of $FeCl_2{\cdot}4H_2O$ and 0.270 g of $FeCl_3{\cdot}6H_2O$ was stirred under constant N_2 bubbling. After 30 min, 50 mL of ammonia (1.5 M) was added to the aqueous solution of iron ions with stirring under N_2 atmosphere at room temperature. The reaction mixture was heated at 70 °C for 1 h (dispersion I). The raw MNCs were collected via filtration and washed with ultrapure water. The MNC-LNT peapod composite was fabricated by adding LNTs into the dispersion I at 50 °C under various pH values (pH 3, 5.4, 6.3, 6.8, 7.8, and 8.9) that were adjusted using 0.1 M HCl. The dispersion was stirred mildly for 3 days.

Characterization. The nanostructure and morphologies of the LNTs and the obtained MNC-LNT peapod composite were observed with a scanning transmission electron microscope (FE-SEM & STEM, Hitachi S-4800) and a transmission electron microscope (TEM, TOPCON EM-002B). For the STEM and TEM observations, a drop of the sample suspension was placed on a carbon-coated copper grid (200 meshes) and dried overnight at room temperature under reduced pressure. The images were taken with the accelerating voltage of 30 kV for FE-SEM and 200 kV for TEM. The X-ray diffraction (XRD) patterns of the prepared raw MNC and the MNC-LNT peapod composite were measured with a Rigaku RINT 2100 diffractometer using Cu Ka radiation set at 1.54 Å, and operated at 40 kV and 30 mA. The zeta potential of the LNT was measured at various pH conditions at 25 °C to evaluate the surface charge of the LNT in aqueous media, with a Malvern Zetasizer Nano-ZS (Malvern Instruments, Malvern, UK). The magnetic properties of the raw MNCs and the MNC-LNT peapod composites were measured at 305 K with a superconducting quantum-interference device (SQUID) magnetometer (Quantum Design, MPMS5S).

Alignment of the MNC-LNT Peapod Composite. The MNC-LNT peapod composites can be aligned in the desired direction by applying an external magnetic field. Two magnets were set at both ends of a slide glass. The dispersion of the composite was dropped on the slide glass. The orientation of the composite with or without the magnetic field was observed with an optical microscope (Leica DMRX). A magnetite nanowire was fabricated by removing the shell of the peapod composite via firing. The drop of the composite dispersion on the silicon wafer was dried under reduced pressure. The dried sample was fired in the air at 300 °C for 30 min to remove the LNT. The morphology of the product was observed via SEM.

RESULTS AND DISCUSSION

Glycolipid (**1**) self-assembles into LNT almost quantitatively in methanol. TEM observation of the LNT showed a homogeneous hollow cylinder with two completely opened ends (Figure 1). Their average inner and outer diameters were 80 and 200 nm, respectively, and their lengths ranged from 0.2 to longer than 60 μm.

The prepared MNCs were 10 nm spherical particles. The X-ray diffraction pattern of the MNC and the MNC-LNT peapod composite, as seen in Figure 2, clearly showed six diffraction peaks that corresponded to the spinel structure of the Fe_3O_4 crystal. Although the XRD patterns of magnetite (Fe_3O_4) and maghemite (γ-Fe_2O_3) were close to each other, the MNCs had the spinel structure of Fe_3O_4 rather than of γ-Fe_2O_3. This is because the characteristic reflection of the (2 2 1), (4 2 1) plane that corresponded to γ-Fe_2O_3 was not observed in the XRD

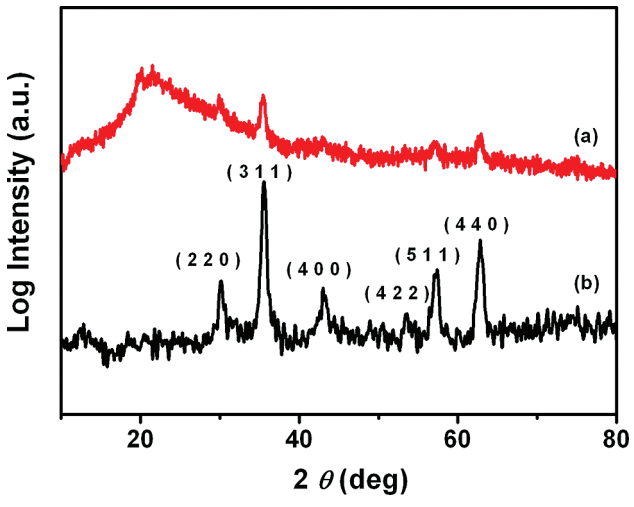

Figure 2. X-ray diffraction pattern of (a) the MNC-LNT peapod composite and (b) the raw MNC.

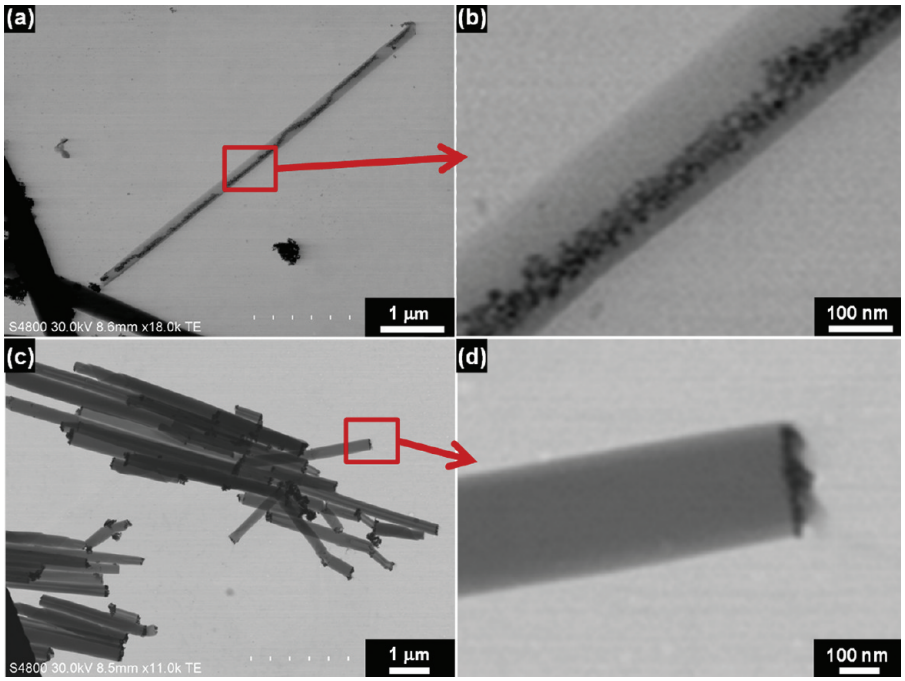

Figure 3. TEM images of the MNC-LNT composites. (a, b) MNC-LNT peapod composite prepared at a pH 6.8 and (c, d) MNC-capped LNT composite prepared at a pH 8.9.

patterns.[27] The additional peaks of the peapod composite near 20° reflect the molecular packing of the lipid alkyl chains of the LNT.[28]

Images a and b in Figure 3 show the FE-STEM images of the MNC-LNT peapod composite that was prepared at a pH of 6.3. The comparison of the SEM and STEM images demonstrated that the MNCs were encapsulated in the LNT (see Figure S1 in the Supporting Information). In the composite, the MNC filled up the LNT hollow cylinder to over 6 μm. This length is longer than that in the previously reported gold-nanocluster- or ferritin-LNT peapod.[8−12] At basic conditions (pH > 7.8), the formation of the MNC-capped LNT composites was observed (Figure 3c,d). Below a pH of 5, the LNT could not be dispersed in the media, and no composite formation was observed.

Figure 4 shows the relationship of the zeta potential of the MNC and the LNT to the pH of the suspension media. The LNT has an iso-electric point (IEP) at ca. pH 3, at which pH it hardly dispersed in the media. The negative zeta potential of the LNT increased with the increase in the pH value. The LNT was well-dispersed in the media at pH ≥5, which has a high absolute value of the zeta potential. On the other hand, the MNC had an IEP at about pH 6.[29] Its zeta potential was negative at pH >6 and positive at pH <6. This may mean that the LNT and the MNC repulse each other at pH >6 and attract at pH 2−6 because of their electrostatic interaction.

The peapod-type composites were formed at the pH values of 5.4−6.8, which was around the IEP of the MNC (see Figure S2 in the Supporting Information). From the results, it was assumed that the MNCs could diffuse into the nanotube hollow cylinder only near the IEP of the MNC. In this pH region, neither a strong attractive nor repulsive electrostatic interaction between the surface of the MNC and the LNT might work due to the low zeta potential of the MNC. Therefore, when LNTs were added in the dispersion of the MNCs, it was thought that the MNCs were drawn into the hollow cavity of the LNTs by

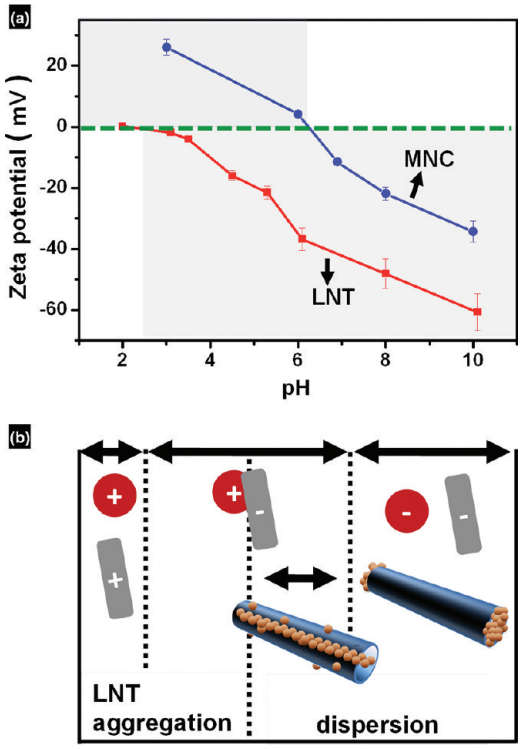

Figure 4. (a) Zeta potential of the MNC and LNT, and (b) schematic of the surface interaction of the MNC and LNT at various pH regions.

the capillary force. It takes longer than 3 days, however, to get an MNC-LNT peapod composite in which the MNC is densely packed. This result meant that the capillary force alone is not enough to form an MNC-LNT peapod composite, since it would finish off the encapsulation of the MNC immediately or at least hours after the addition of the LNT. The manner of the diffusive entrance of the MNCs into the LNT can be explained

dx.doi.org/10.1021/am300122f | ACS Appl. Mater. Interfaces 2012, 4, 2439−2444

by the following two characteristics of the water in the glucose-based LNT.[30] First, the polarity of the water in the LNT was lower than that in the bulk. Second, the viscosity of the water in the LNT was higher than that in the bulk. The MNCs with a low zeta potential prefer to be in the less polar hollow region of the LNT due to their hydrophobicity.[31] Also, the MNCs would be slowly diffused along the LNT axis, since the water in the LNT is more viscous than the bulk water. Moreover, the diffusional movements of the MNCs inside and outside the LNT may differ much because the tubular structure provides the MNCs with a limited space for movement.[32]

Above a pH of 7.8, both the LNT and the MNCs have a high negative zeta potential. It was expected that their strong electrical repulsion would overcome the capillary and diffusion force, so that no composite would be formed. Contrary to this expectation, the MNCs and the LNT formed MNC-capped composites in a pH 7.8 and a pH 8.9 (see Figure S3 in the Supporting Information). The reason for the aggregation of the MNCs at the end of the LNT is still unclear. The following explanations were assumed, though. First, the electrostatic interaction between the MNCs and the LNT prevented the diffusion of the MNCs into the nanotube hollow cylinder. Second, at the end of the LNT, the amide group of the glycolipid that electrostatically interacted with the MNCs might have been exposed to the media.[33] The amide functional group of the glycolipid has electron-rich oxygen and electron-deficient hydrogen that induce the preferable adsorption of the MNCs at the end of the LNT. On one hand, it was thought that this interaction could act as a force for gathering the MNCs near the entrance of the LNT. This could have contributed to the dense packing of the MNC-LNT peapod composites at the pH range of 5.4−6.8 because the gathered MNCs could be diffused into the LNT more easily than when they are dispersed in the solution.

The diffused MNCs were not eluted out of the magnetite peapod composite after dilution or drying. The different property of the water in the hollow of the LNT resulted from the hydrogen bond of the water molecules and the abundant sugar OH groups that covered the inner surface of the LNT.[30] Therefore, it could also be suggested that the MNCs were bound by the hydrogen bond in the inner surface of the LNT.

According to literature, for 1-D anisotropic magnetic materials, the coercivity (H_c) in the parallel magnetic field is higher than that in the perpendicular magnetic field.[34,35] In terms of the anisotropicity and isotropicity of the MNCs, the H_c of the isotropic MNCs is lower than that of the anisotropic MNCs in the parallel magnetic field and higher than that in the perpendicular magnetic field. The magnetic properties of anisotropic magnetic materials are considered to be influenced by different factors such as their shape anisotropy, magneto-crystalline anisotropy, and dipolar interaction.[36] Because the magnetocrystalline anisotropy depends only on the micro-structure of the particle, the energy could be ignored for the peapod composite of the 1D arrangement of the MNC. The large shape anisotropy of the composite, however, could affect its magnetic property. It contributed to the higher coercivity of the peapod composite. It was known that ferromagnetic coupling in a uniaxial chain such as in a particle system increases the coercivity.[37−39] This is because the direction of the magnetic dipole moment interaction between the adjacent particles is uniform in the anisotropic MNC arrangement, whereas the direction of the interaction is random in the isotropic arrangement.

In Figure 5, the resulting magnetic moment M of the raw MNC and the MNC-LNT peapod composite are plotted against the magnetic field H at 305 K, measured via SQUID. The hysteresis loop of the raw MNC is narrower than that of the peapod composite. The magnetic saturation values of the raw MNCs and the MNC-LNT peapod composites are 69.9 and 7.9 emu/g, respectively. The lower magnetic saturation value in the MNC-LNT peapod composite than that in the raw MNC is due to the small content of the MNC in the peapod composite. The amount of the MNCs occupied in the LNT was small because the hollow space of the LNT is limited. The remanence and coercivity (H_c) of the raw MNCs are 1.0 emu/g and 5.8 Oe, respectively. Those of the MNC-LNT peapod composites are 0.1 emu/g and 10.6 Oe, respectively. The H_c of the peapod is larger than that of the raw MNC. 1D magnetic material has shown an increase of the coercivity when it was exposed in the parallel magnetic field.[34,35] Thus, the increase in coercivity indicates that the peapod was aligned randomly, but a part of the peapod was aligned in the direction of the applied magnetic field and enhanced the H_c.

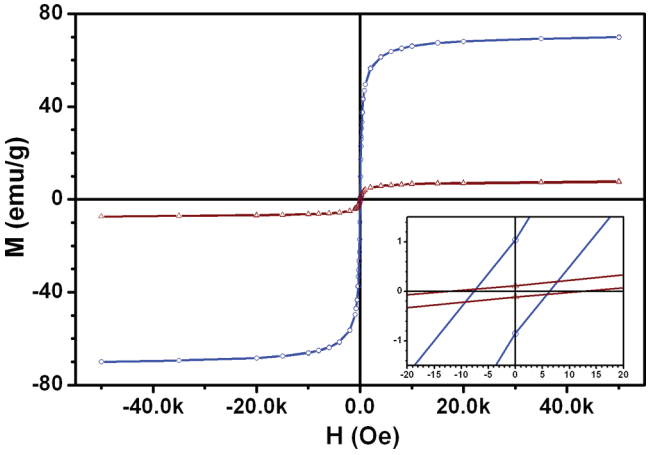

Figure 5. Room-temperature hysteresis loops of (a) the raw MNC and (b) the MNC-LNT peapod composite. Inset: magnification to confirm the change in the coercivity.

Magnetic materials whose coercivities range from 10 to 100 Oe are called "semi-hard" magnetic materials.[4042] Such magnetic materials are suitable as magnetic recording materials. The magnetic property of the MNC changes from "soft" to "semi-hard" with the peapod formation. If all the peapods in the sample align in the applied magnetic field, their magnetic property will be "harder" than that of the randomly aligned peapods.

The MNC-LNT peapod composites can be aligned in the desired direction by applying an external magnetic field to fabricate a magnetite nanowire through removal of the shell of the peapod composite via firing. In the magnetic field, the composite was oriented parallel to the applied external magnetic field, and its body was stretched (Figure 6a). Also, the SEM observation after the LNT removal via firing confirmed the parallel arrangement of the MNCs to the magnetic field (Figure 6c). When there was no external magnetic field, the composites in the fluid showed an entangled pattern of the winding fiber (Figure 6b), and the firing left only aggregated MNCs with a disordered pattern (Figure 6d).

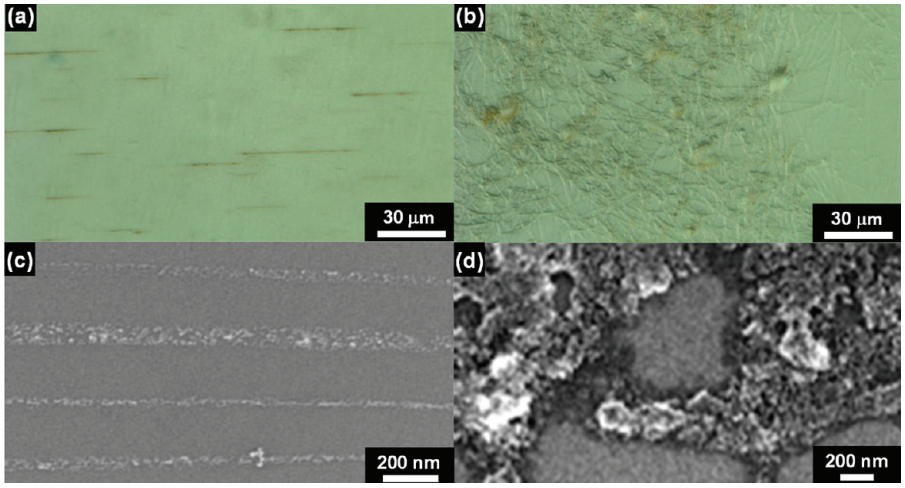

Figure 6. Optical micrographs (top) and SEM images (bottom) of the MNC-LNT peapod composite after it was fired in the air at 300 °C (a, c) in the external magnetic field and (b, d) without the magnetic field.

CONCLUSION

In this work, we achieved anisotropic 1D arrangement of the MNCs through the formation of the MNC-LNT peapod composites by simple mixing the MNCs and LNT. Although a capillary force could not be ignored as a driving force to put the MNCs into LNT, it was clear that the adjustment of the surface electrostatic interaction was important to prepare a densely packed MNC-LNT peapod composite. Experimentally, it was assumed that the interaction was small at pH 5.4−6.8 around IEP of the MNC, and the formations of the peapod composites were confirmed. Further it was discussed that the different condition of the inner side and outer side of LNT such as polarity and viscosity of water was aid in diffusing the MNCs into LNT. Also, it should be noted that the coercivity of the MNC was enhanced by the peapod formation. These composites can be aligned in desired direction by applying external magnetic field. This work will certainly lead to a simple and mild approach for the fabrication and the arrangement of the 1D nanocomposites of magnetic materials. When this composite was hybridized with other materials, its magnetic property will be useful for the preparation of nanodevices.

ASSOCIATED CONTENT

Supporting Information

FE-STEM images of the peapod composite prepared at a pH 5.5, 6.3, 6.8, and 7.8. This material is available free of charge via the Internet at http://pubs.acs.org/.

AUTHOR INFORMATION

Corresponding Author

*Fax: +81-29-861-4461. Tel.: +81-29-861-4676. E-mail: han-119@aist.go.jp (Y.-G.H.); masaru-aoyagi@aist.go.jp (M.A.).

Notes

The authors declare no competing financial interest.

ACKNOWLEDGMENTS

The authors thank Dr. Kenji Kawaguchi (AIST, Ibaraki, Japan) for the magnetization experiments. The financial support of the innovation school program of AIST is also acknowledged.

REFERENCES

(1) Kamiya, S.; Minamikawa, H.; Jung, J. H.; Yang, B.; Masuda, M.; Shimizu, T. *Langmuir* **2005**, *21*, 743−750.
(2) Singh, A.; Schnur, J. M. *Synth. Commun.* **1986**, *16*, 847−852.
(3) Kogiso, M.; Aoyagi, M.; Asakawa, M.; Shimizu, T. *Soft Matter.* **2010**, *6*, 4528−4535.
(4) Shimizu, T.; Masuda, M.; Minamikawa, H. *Chem. Rev.* **2005**, *105*, 1401−1444.
(5) Schnur, J. M.; Price, R.; Rudolph, A. S. *J. Controlled Release* **1994**, *28*, 3−13.
(6) Spargo, B. J.; Cliff, R. O.; Rollwagen, F. M.; Rudolph, A. S. *J. Microencapsul.* **1995**, *12*, 247−254.
(7) Meilander, N. J.; Pasumarthy, M. K.; Kowalczyk, T. H.; Cooper, M. J.; Bellamkonda, R. V. *J. Controlled Release* **2003**, *88*, 321−331.
(8) Kameta, N.; Masuda, M.; Minamikawa, H.; Mishima, Y.; Yamashita, I.; Shimizu, T. *Chem. Mater.* **2007**, *19*, 3553−3560.
(9) Yang, B.; Kamiya, S.; Yoshida, K.; Shimizu, T. *Chem. Commun.* **2004**, 500−501.
(10) Yang, B.; Kamiya, S.; Shimizu, Y.; Koshizaki, N.; Shimizu, T. *Chem. Mater.* **2004**, *16*, 2826−2831.
(11) Yui, H.; Shimizu, Y.; Kamiya, S.; Masuda, M.; Yamashita, I.; Ito, K.; Shimizu, T. *Chem. Lett.* **2005**, *34*, 232−233.
(12) Shimizu, T. *J. Polym. Sci., Part A: Polym. Chem.* **2008**, *46*, 2601−2611.
(13) Reich, S. *J. Mater. Sci.* **1987**, *22*, 3391−3394.
(14) Liu, C.-P.; Wang, R.-C.; Kuo, C.-L.; Liang, Y.-H.; Chen, W.-Y. *Rec. Pat. Nanotechnol.* **2007**, *1*, 11−20.
(15) Huang, Y.; Duan, X.; Wei, Q.; Lieber, C. M. *Science* **2001**, *291*, 630−633.
(16) Liu, J.; Gao, P.; Mai, W.; Lao, C.; Wang, Z. L. *Appl. Phys. Lett.* **2006**, *89*, 063125.
(17) Zhang, L.; Lan, T.; Wang, J.; Wei, L.; Yang, Z.; Zhang, Y. *Nanoscale Res. Lett.* **2011**, *6*, 58.
(18) Zhang, L. Y.; Xue, D. S.; Xu, X. F.; Gui, A. B. *J. Magn. Magn. Mater.* **2005**, *294*, 10−15.
(19) de Araújo, A. E. P.; Duque, J. G. S.; Knobel, M.; Schnitzler, M. C.; Zarbin, A. J. G. *J. Magn. Magn. Mater.* **2007**, *312*, 32−34.
(20) Cui, Y.; Zhong, Z. H.; Wang, D. L.; Wang, W. U.; Lieber, C. M. *Nano Lett.* **2003**, *3*, 149−152.
(21) Huang, M. H.; Mao, S.; Feick, H.; Yan, H. Q.; Wu, Y. Y.; Kind, H.; Weber, E.; Russo, R.; Yang, P. D. *Science* **2001**, *292*, 1897−1899.
(22) Hochbaum, A. I.; Chen, R. K.; Delgado, R. D.; Liang, W. J.; Garnett, E. C.; Najarian, M.; Majumdar, A.; Yang, P. D. *Nature* **2008**, *451*, 163−167.
(23) Cho, E. C.; Shim, J.-W.; Lee, K. E.; Kim, J.-W.; Han, S. S. *ACS Appl. Mater. Interfaces* **2009**, *1*, 1159−1162.

(24) Han, Y.-G.; Aoyagi, M.; Kogiso, M.; Asakawa, M.; Shimizu, T. *Colloid. Surface Physicochem. Eng. Aspect* **2012**, *395*, 63−69.
(25) U.S. Patent 3 843 540, 1974.
(26) Ramirez, L. P.; Landfester, K. *Macromol. Chem. Phys.* **2003**, *204*, 22−31.
(27) Chakrabarti, S.; Mandal, S. K.; Nath, B. K.; Das, D.; Ganguli, D.; Chaudhuri, S. *Eur. Phys. J. B* **2003**, *34*, 163−171.
(28) Yui, H.; Minamikawa, H; Danev, R.; Nagayama, K; Kamiya, S; Shimizu, T. *Langmuir* **2008**, *24*, 709−713.
(29) Parks, G. A. *Chem. Rev.* **1965**, *65*, 177−198.
(30) Yui, H.; Guo, Y.; Koyama, K.; Sawada, T.; John, G.; Yang, B.; Masuda, M.; Shimizu, T. *Langmuir* **2005**, *21*, 721−727.
(31) Fukuzaki, S.; Urano, H.; Nagata, K. *J. Ferment. Bioeng.* **1995**, *81*, 163−167.
(32) Wang, Z.; Sheetz, M. P. *Cell Struct. Funct.* **1999**, *24*, 373−383.
(33) Samba Sivudu, K.; Rhee, K. Y. *Colloids Surf., A* **2009**, *349*, 29−34.
(34) Sharma, N.; Jaffari, G. H.; Shah, S. I.; Pochan, D. J. *Nanotechnology* **2010**, *21*, 085707.
(35) Russier, V.; Petit, C.; Pileni, M. P. *J. Appl. Phys.* **2003**, *93*, 10001−10010.
(36) Sellmyer, D. J.; Zheng, M.; Skomski, R. *J. Phys.: Condens. Matter.* **2001**, *13*, R433−R460.
(37) Zhang, L.; Manthiram, A. *Phys. Rev. B* **1996**, *54*, 3462−3467.
(38) Tsang, S. C.; Chen, Y. K.; Harris, P. J. F.; Green, M. L. H. *Nature* **1994**, *372*, 159−162.
(39) Dujardin, E.; Ebbesen, T. W.; Hiura, H.; Tanigaki, K. *Science* **1994**, *265*, 1850−1852.
(40) Ault, C. F.; Gallagher, L. E.; Greenwood, T. S.; Kohler, D. C. *Bell System Tech. J.* **1964**, *43*, 2097−2146.
(41) Chin, G. Y. *J. Magn. Magn. Mater.* **1978**, *9*, 283−298.
(42) Nesbitt, E. A.; Chin, G. Y.; Jaffe, D. *J. Appl. Phys.* **1968**, *39*, 1268−1269.